

## Isotherm, Kinetic and Thermodynamic Investigation into Methylene Blue Adsorption onto Pinecone Powder

Adnan Aldemir<sup>1,\*</sup>, Ali Rıza Kul<sup>2</sup>, Hasan Elik<sup>2</sup>

<sup>1</sup>Van Yüzüncü Yıl University, Faculty of Engineering, Chemical Engineering Department, 65080, Van, Turkey;

<sup>2</sup>Van Yüzüncü Yıl University, Faculty of Science, Chemistry Department, 65080, Van, Turkey

Received September 18, 2019; Acceptor December 3, 2019

**Abstract:** In this study, the usage of pine cone powder as an adsorbent for removing methylene blue from aqueous solution was investigated. Within this scope adsorption experiments were performed, and the results showed that the Freundlich isotherm model was a more convenient option compared to the Langmuir and Temkin models. The results also determined that the pseudo second order kinetic model demonstrated higher correlation coefficients ( $R^2$ ) values compared to the pseudo first order and intra-particle diffusion models. Initial dye concentration was found to shift from 100 to 300 mg/L, while adsorption capacity onto the pine cone powder changed from 40.99 to 95.24 mg/g, 41.56 to 97.93 mg/g, and 43.51 to 101.41 mg/g for 298K, 308K and 318K, respectively. The thermodynamic parameters for the instant free energy ( $\Delta G$ ), enthalpy ( $\Delta H$ ), and entropy ( $\Delta S$ ) of this separation process were found by referring to -1595,11 J/mol, 2465,83 J/mol and 12,77J/mol, respectively. The negative  $\Delta G^\circ$  values revealed that this separation process was endothermic and natural.

**Keywords:** *adsorption, isotherm, kinetic, thermodynamic, pine cone, methylene blue*

### Introduction

Various methods based on the chemical structure, colour and application are available to classify commercial dyes. As for the chemical structure classes, the dyes utilized industrially are the anthraquinone, azo, indigoid, phthalocyanine, sulphur, and triphenylmethyl (trityl) (Gupta & Suhas, 2009; Yagub *et al.*, 2014). Quaternary salts are classified as basic dyes. Their cations have a positive charge mostly on nitrogen (N), carbon(C), oxygen(O) and sulphur(S) atoms while their anions are mostly  $Cl^-$ ,  $SO_4^{2-}$ ,  $HSO_4^-$  or  $(COO^-)_2$  ions (Forgacs *et al.*, 2004; Yagub *et al.*, 2014).

Dyes have a stable and complex structure and a slow biodegradability. They are toxic to the organisms in the receiving waters and negatively affect the photosynthetic activities in such waters. The different dye classes and their health effects are given in (Kausar *et al.*, 2018). Due to their harmful effects on the human beings, dyes must be removed from the aqueous solutions.

To date, several chemical and biological treatment methods, including electrocoagulation and chemical oxidation have been applied in the treatment of industrial wastewaters (Mahmodi *et al.*, 2011; Debnath *et al.*, 2017). Among these methods, the adsorption technique with relatively economical, efficient, flexible, and simple design has proved to ensure operational comfort in treating colorized wastewaters (Mtshatsheni *et al.*, 2019). The performance of the adsorption technique is associated with the adsorbent materials. Activated carbon, a commonly used adsorbent, is very expensive, has high operation costs and requires regeneration after the treatment process (Jin *et al.*, 2019). This limitation has to evoke a search for different adsorbents, such as biosorbents and waste materials to be used in the removal of dyes. Natural wastes have been used as adsorbents in the removal of dyes from wastewaters as they are low in cost, efficient, locally available materials and not hazardous to nature (Salleh *et al.*, 2011; Crini, 2006).

Pine cones are important commercial and value and used extensively in many different industries (Martin-Lara *et al.*, 2016). One pine cone consists of around 46.5% hemicellulose, 37.4% lignin, 18.8% cellulose, and 15.4% extractives (Ofomaja *et al.*, 2010). Pine cone powder (PCP) has been used for remove the heavy metal pollutants such as lead, caesium, copper, nickel, and arsenic (Immaculate *et al.*, 2018). There are only a limited number of studies that have been conducted on the dye adsorption capacity of these species (Mahmodi *et al.*, 2011). The present study investigated the dye adsorption capacity of PCP. Various adsorbents have been investigated for the adsorption of MB

\*Corresponding: E-Mail: [adnanaldemir@yyu.edu.tr](mailto:adnanaldemir@yyu.edu.tr); Tel: +904322251725 Fax: +904324865413

onto aqueous solutions. As a result, some of them provided well-suited MB adsorption properties (Kul & Aldemir, 2019).

The interference between the adsorbent and adsorbate molecules is explained by way of adsorption isotherms. The adsorbate nature alters the amount adsorbed and the adsorbent affects the adsorption isotherm profile shape. In the present study, all of the above-mentioned isotherms were taken into account. The assumption with the Langmuir isotherm model, is that the adsorption onto the monolayer and all the active sites on the adsorbent surface are equal in terms of energy. The Freundlich isotherm model, on the other hand clarifies the multilayer adsorption behaviour. The kinetic mechanism of the adsorption process is explained by calculating different equations such as pseudo first order (PFO), pseudo second order (PSO) and intra-particle diffusion (IPD) models (Ofomaja *et al.*, 2010).

In this study, the adsorption capacity of PCP onto MB was evaluated. Several parameters, important for dye removal were investigated within scope. MB was selected as the adsorbate due to it is being considered a toxic dye.

## Materials and Methods

### The Adsorbent (Pine Cone Powder)

The adsorption experiments were carried out using PCP obtained from *Pinus sylvestris* grown in the province Van in Turkey. After being collected the pine cones were washed multiple times using distilled water to remove any impurities. They were dried in an oven at 55 °C for 48h. The dried pine cones were later ground in a crusher. The resulting powders were sieved and the particles that measured less than 150 µm were gathered together in a plastic container to be used as adsorbents.

### The Adsorbate (Methylene Blue)

In this study MB was used as the adsorbate. The formula of MB which has a molecular weight of 319.85 g/mol, is  $C_{16}H_{18}N_2S_2Cl_2 \cdot 3H_2O$ . The dye was purchased from Merck Chemicals Company (Germany) and used without any purification processes. The stock dye solution was prepared by dissolving 1 g of MB in 1000 ml of distilled water. The dye solutions (100-300 mg/L) used in the adsorption process were acquired by diluting the prepared stock dye solution with deionized water to the appropriate concentrations.

### Adsorption Experiments

2 g of adsorbent treated with 500 ml of dye solution in a batch temperature-controlled water bath. Different initial concentrations of MB were available in the dye solution during 120 min while the pH was gradually adjusted with the addition of either  $H_2SO_4$  solution or NaOH solution (0.1 M) to keep the constant pH values. All triplicate experiments were executed under the same conditions at temperatures of 298K, 308K and 318K. Consequently, average values were taken as the result after the entire data was calculated. Adsorption capacity was calculated with Eq. (1);

$$q_e = \frac{(C_0 - C_e)V}{m} \quad (1)$$

where V is the volume of the solution (L),  $C_0$  and  $C_e$  are the initial and the equilibrium concentration of the dye (mg/L), respectively and m is the adsorbent mass (g). The data obtained in this study were tested by isotherm, kinetic and thermodynamic relationships to design the most appropriate MB removal conditions using PCP.

## Results and Discussion

### Adsorption Isotherm Studies

Many different models are used in identifying the adsorption of dyes onto solid surfaces. Three models were applicable to the descriptions of the experimental results obtained at three different temperatures. The parameters of these isotherm models were considered through regression by means of the linear isotherm equations (Mahmodi *et al.*, 2011; Rida *et al.*, 2013). The amount of the MB adsorbed for three temperatures are presented in Figure 1. The adsorption efficiency increases as the initial MB concentration rises.

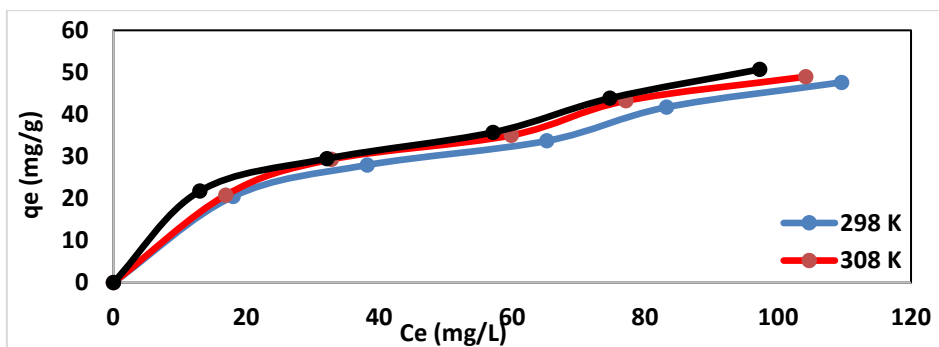


**Figure 1.** MB adsorption isotherms onto PCP at different temperatures

The Langmuir isotherm equation is given with Eq. (2);

$$q_e = \frac{q_m K_L C_e}{1 + K_L C_e} \tag{2}$$

where  $q_{max}$  is the maximum adsorption capacity (mg/g),  $C_e$  is the equilibrium concentration of the solution (mg/L), and  $K_L$  is a Langmuir constant. The values of  $q_m$  and  $K_L$  are determined by using the slope and intercept of the graph of  $C_e/q_e$  versus  $C_e$ . Figure 2 shows the isotherm results of MB adsorption onto PCP for 298K, 308K, and 318 K.

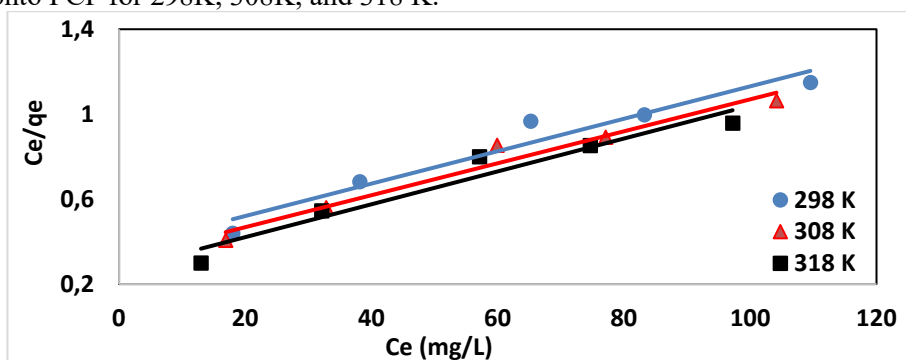


**Figure 2.** Langmuir isotherms of MB adsorption onto PCP for different temperatures

The Freundlich isotherm equation is given with Eq. (3);

$$q_e = K_F C_e^{1/n} \tag{3}$$

where  $K_F$  is a Freundlich constant associated with the adsorption capacity (L/g) and  $1/n$  is an empirical parameter associated with the adsorption intensity. Figure 3 shows the Freundlich isotherm results of MB adsorption on PCP for 298K, 308K, and 318 K.

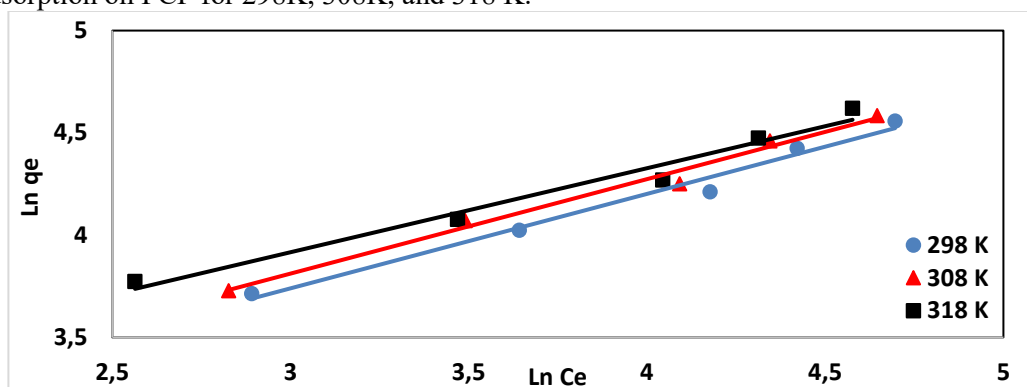


**Figure 3.** Freundlich isotherms of MB adsorption onto PCP for different temperatures

The Temkin isotherm equation is given with Eq. (4);

$$q_e = \frac{RT}{b_T} \ln K_T + \frac{RT}{b_T} \ln C_e \tag{4}$$

where  $K_T$  and  $b_T$  are both related to the adsorption heat. Figure 4 shows the Temkin isotherm results of MB adsorption onto PCP for 298K, 308K, and 318 K.

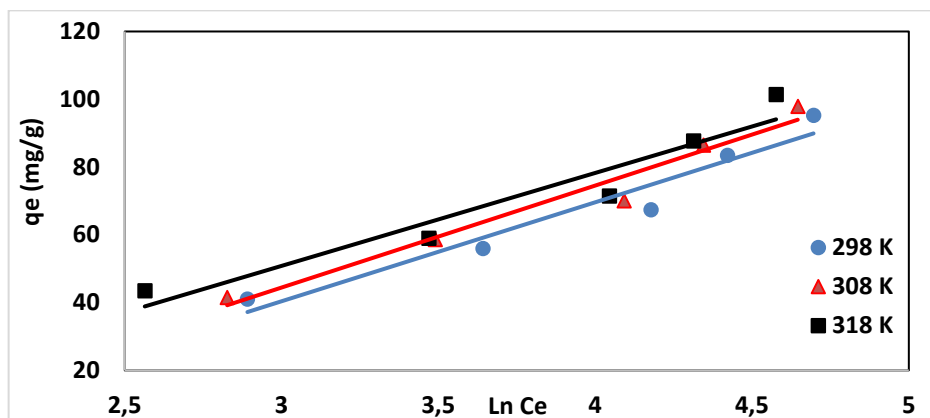


**Figure 4.** Temkin isotherms of MB adsorption onto PCP for different temperatures

The parameters calculated for MB adsorption onto PCP are presented in Table 1. With respect to the determined coefficients it was determined that the Freundlich model was more suitable than both the Langmuir model and the Temkin model. It was found that the values of  $K_F$  and  $n$  increased with the increase in temperature and that adsorption was accomplishable at higher temperatures. The  $R^2$  values of all three isotherm models were high however the  $R^2$  values of the Freundlich model were higher than those of the other two models. Table 2 shows the maximum adsorption capacity ( $q_m$ ) of MB for different adsorbents while Table 3 shows pine cone adsorbent with different adsorbates calculated according to Langmuir isotherm model.

**Table 1.** Isotherm model parameters for MB adsorption on PCP at different temperatures

| Temp<br>K | Langmuir         |                 |        | Freundlich |                |        | Temkin         |                  |        |
|-----------|------------------|-----------------|--------|------------|----------------|--------|----------------|------------------|--------|
|           | $K_L$<br>(L / g) | $q_m$<br>(mg/g) | $R^2$  | $n$        | $K_F$<br>(L/g) | $R^2$  | $K_T$<br>(L/g) | $b_T$<br>(J/mol) | $R^2$  |
| 298       | 0.0208           | 65.359          | 0.9436 | 0.4085     | 5.2683         | 0.9922 | 1.6162         | 169.734          | 0.9409 |
| 308       | 0.0236           | 66.667          | 0.9633 | 0.4617     | 5.6604         | 0.9961 | 1.5223         | 180.258          | 0.9606 |
| 318       | 0.0291           | 68.516          | 0.9386 | 0.5109     | 7.3251         | 0.9947 | 1.2718         | 192.841          | 0.9221 |

### Effect of Temperature and Thermodynamics on Adsorption

The effect of temperature on MB adsorption was investigated by conducting experiments at three different temperatures. The experimental results showed that MB adsorption capacity decrease when temperature increased. This was caused by the adsorbed MB ions escaping which indicates the physical nature of the adsorption. Thermodynamic parameters are extremely important in detecting heat alteration in the adsorption process for the dye and PCP (Debnath *et al.*, 2017). These parameters were calculated by using the following equations:

$$K_C = \frac{C_{Ads}}{C_e} \tag{5}$$

$$\Delta G^\circ = -RT \ln K_C \tag{6}$$

$$\Delta G^\circ = \Delta H^\circ - T \Delta S^\circ \tag{7}$$

$$\ln K_C = \frac{\Delta S^\circ}{R} - \frac{\Delta H^\circ}{RT} \tag{8}$$

where  $C_{Ads}$  is the dye amount (mg) adsorbed onto PCP per liter of the solution in equilibrium, the adsorbent per unit liter of the solution. Figure 5, shows the straight line, namely  $\ln K_C$  versus  $1/T$ , obtained from the graphical representation in accordance with Eq. (8). The thermodynamic parameters are given in Table 4.

**Table 2.** Adsorption capacity of MB onto different adsorbents

| Adsorbent                                    | $q_m$ (mg/g) | References                |
|--|--------------|---------------------------|
| NaOH treated diatomite                       | 27.8         | (Cherifi et al., 2013)    |
| Fe <sub>3</sub> O <sub>4</sub> nanoparticles | 38.2         | (Gouamid et al., 2013)    |
| Vegetal fiber activated carbons              | 33.7         | (Caparkaya et al., 2008)  |
| Date palm leaves powder                      | 58.1         | (El Sikaily et al., 2006) |
| The brawn algae                              | 38.6         | (Fu et al., 2000)         |
| The green algae                              | 40.2         | (Dawood et al., 2012)     |
| Dead fungus                                  | 18.5         | (Ofomaja et al., 2010)    |
| Marble dust                                  | 16.3         | (Hamed et al., 2014)      |
| PCP  | 68.5         | This study                |

**Table 3.** Monolayer capacity of natural PCP on various adsorbates

| Adsorbate       | $q_m$ (mg/g) | References                |
|-----------------|--------------|---------------------------|
| Acid Blue 7     | 37.4         | (Mahmudi et al., 2011)    |
| Acid Green 25   | 43.3         | (Mahmudi et al., 2011)    |
| Acid Black 26   | 62.9         | (Mahmudi et al., 2011)    |
| Congo Red       | 32.6         | (Demirak et al., 2015)    |
| Pb(II) metal    | 16.3         | (Kul and Koyuncu, 2010)   |
| Cu(II) metal    | 9.22         | (Ofomaja et al., 2009)    |
| NH <sub>4</sub> | 6.15         | (Rafatullah et al., 2010) |
| 2-nitrophenol   | 41.17        | (Kupeta et al., 2018)     |
| Methylene Blue  | 68.5         | This study                |

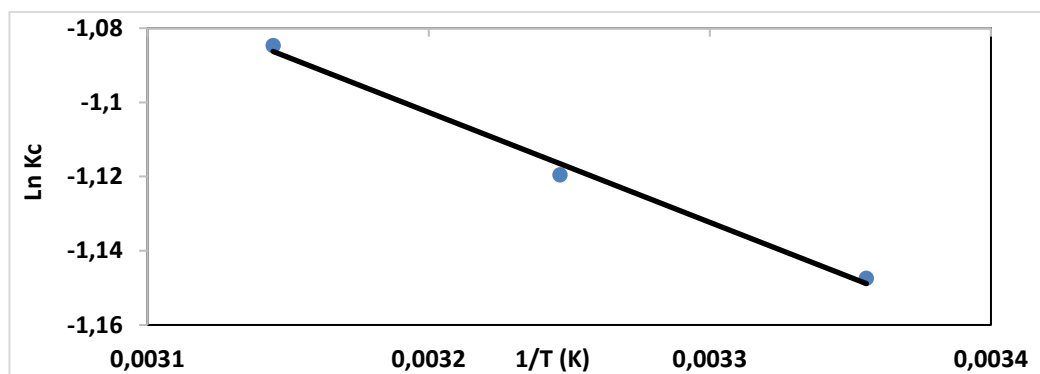


**Figure 5.**  $\ln K_c$  versus  $1/T$  plot for MB adsorption onto PCP

The Gibbs free energy ( $\Delta G^\circ$ ) absolute values of MB adsorption onto PCP were obtained as -1,3396 kJ/mol, -1,4673 kJ/mol, and -1,5951 kJ/mol for 298K, 308K, and 318K, respectively. The enthalpy ( $\Delta H^\circ$ ) and entropy ( $\Delta S^\circ$ ) values of MB adsorption onto PCP were found to be 2465.81 J/mol and 12.77 J/mol.K, respectively.

The values of  $\Delta H^\circ$  were found to be within the range of 1–60 kJ/mol which indicated physical adsorption. Physical adsorption can be the result of Van der Waals forces and/or weak charge transfer complexes between the adsorbate and adsorbent (Kupeta *et al.*, 2018). From the results obtained, it can clearly be seen that physical adsorption is favourable for the adsorption of MB. The positive values of  $\Delta H^\circ$  proved the endothermic nature of the adsorption which governs the possibility of physical adsorption. The low value of  $\Delta H^\circ$  suggested that MB is physisorbed onto PCP while the negative values of  $\Delta G^\circ$  showed that the adsorption is spontaneous and extremely favorable. The positive values of  $\Delta S^\circ$  exhibited the increased disorder and randomness at the solid solution interface of MB with PCP adsorbent that causes various structural changes in MB and PCP (Miyah *et al.*, 2018).

**Table 4.** Thermodynamic parameters of MB adsorption onto the PCP

| Temp (K) | Kc    | $\Delta G^\circ$ (kJ/mol) | $\Delta H^\circ$ (kJ/mol) | $\Delta S^\circ$ (J/mol.K) | R <sup>2</sup> |
|----------|-------|---------------------------|---------------------------|----------------------------|----------------|
| 298      | 0.317 | -1.3396                   |                           |                            |                |
| 308      | 0.327 | -1.4673                   | 2.4658                    | 12.7703                    | 0.993          |
| 318      | 0.337 | -1.5951                   |                           |                            |                |

### The Contact Time on Dye and Initial Dye Concentrations

As can be seen from Figures 6, 7 and 8, the removal of MB from the solutions is rapid in the initial period while this speed decreases in the final period in the near reach of the balance. At the start, the surface of adsorption is large and thus, the adsorption onto this surface is rapid. Figure 6, 7 and 8 show that the increase in the initial MB concentration leads to an increase in the adsorption capacity for all three temperatures. As the initial dye concentration increased from 100 to 300 mg/L, the dye adsorption capacity onto the PCP instead from 40.99 to 95.24 mg/g for 298K, 41.56 to 97.93 mg/g for 308K and 43.51 to 101.41 mg/g for 318K. These data prove that the initial dye concentration plays a crucial role in dye adsorption capacity and provides a driving power in the interaction between the adsorbent and the dye. MB adsorption on PCP has similarity herewith. Various studies in the literature have investigated the usage of different adsorbents and biosorbents, such as activated carbon, breadnut skin, hydrochar, rice husk, and sawdust for MB adsorption. When the results of these studies and those of the present study are compared it can be said that dye adsorption capacity of PCP is good and PCP may be the answer to a new inexpensive adsorbent usable for dye removal.

Figure 6, 7 and 8 are shows the changes of  $q_e$  (mg/g) versus time with nearly 50 min response times. Indeed, this can be explained by the fact that the migration of the dye solution can easily accessible to the vacant sites of the adsorbent in the initial period. Thus, a higher adsorption percentage is a result of the gradient concentration of the solid-liquid interface. The gradient concentration is extremely high at the beginning of contact between the solid and liquid phases. However, in the next period adsorption decreases due to the slower diffusion of the dissolved species through the adsorbent pores. The rapid removals of dyes facilitate the use of the decreased adsorbent amounts and thus ensure the efficiency and cost of separation (Miyah *et al.*, 2018).

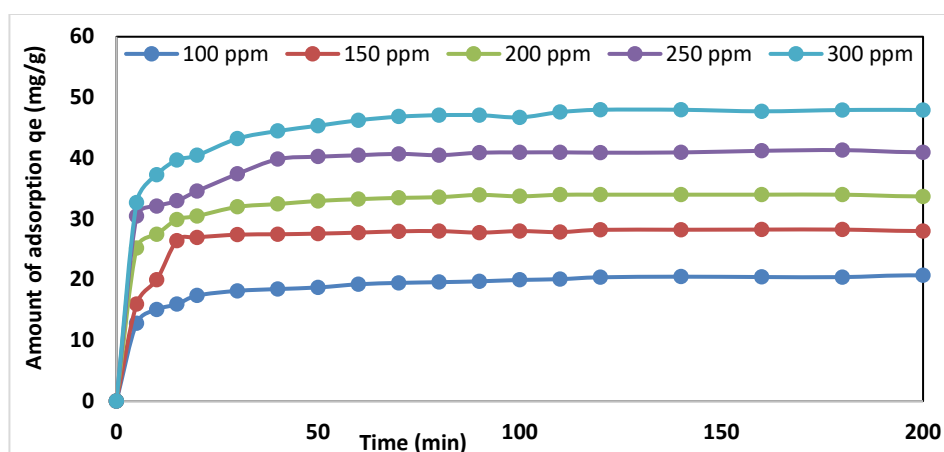


**Figure 6.** Effect of contact time and initial concentration on MB removal onto PCP at 298 K

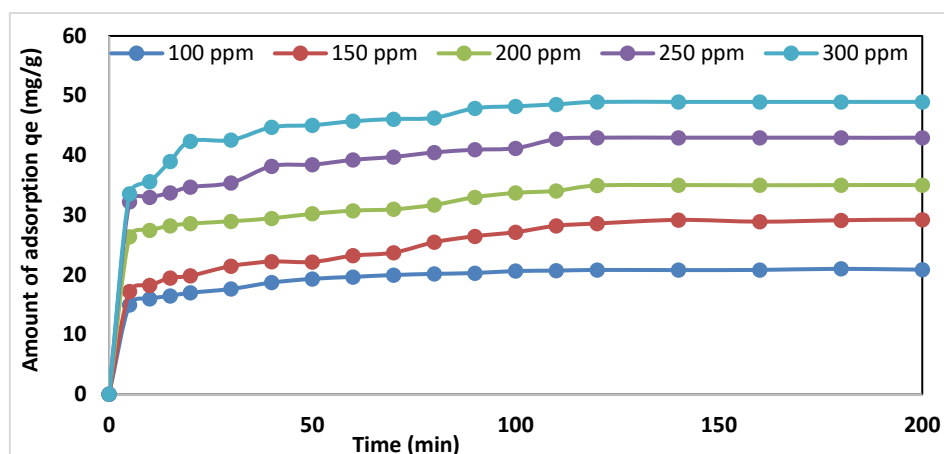


**Figure 7.** Effect of contact time and initial concentration on MB removal onto PCP at 308 K

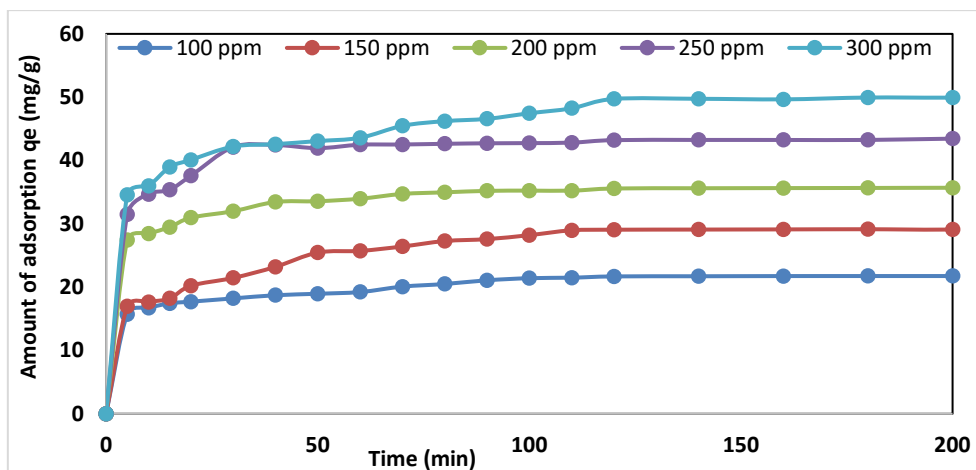


**Figure 8.** Effect of contact time and initial concentration on MB removal onto PCP at 318 K

### Kinetics Studies for Adsorption

Kinetic models are used to evaluate the experimental results of the adsorption of adsorbates onto adsorbents. The adsorption kinetics of dyes is important when choosing the best test circumstances. Useful kinetic parameters for estimating adsorption rates provide vital knowledge to design and modelling adsorption processes (Jian *et al.*, 2013). In the present study, MB was calculated by using three kinetic models, namely (PFO, PSO, and IPD). The most suitable model was chosen depending on the linear regression coefficient of the correlation coefficients of the  $R^2$  values. All three models were examined in accordance with the experimental data at three temperatures and initial MB concentrations (Mahmodi *et al.*, 2011).

The PFO kinetic model separates the kinetics equation according to the solution concentration and solid adsorption capacity. This model is most likely the first to characterize liquid-solid adsorption systems depending on solid capacity. It is utilized for studying the sorption in a liquid-solid system (Ghaedi *et al.*, 2015). The equation of the model is given with Eq. (9);

$$\ln(q_e - q_t) = \ln q_e - k_1 t \tag{9}$$

where  $q_m$  (mg/g) is the adsorption capacity in equilibrium,  $q_t$  (mg/g) is the adsorption capacity at time  $t$ , respectively and  $k_1$  ( $\text{min}^{-1}$ ) is the rate constant of the PFO adsorption. To acquire the constants of this model the straight-line plots of  $\ln(q_e - q_t)$  versus  $t$  are drawn. The constants are determined from the slope and intercept of the plot.

The fitness between the experimental data and the model-predicted values was expressed with the correlation coefficients ( $R^2$ ) and the closeness of the experimental and theoretical adsorption capacity values. The PSO model was found to be successful in representing the kinetics of several adsorption systems (Hamed *et al.*, 2014). The equation for this kinetic model, which is based on adsorption capacity is given with Eq. (10);

$$\frac{t}{q_t} = \frac{1}{k_2 q_e^2} + \frac{1}{q_e} t \tag{10}$$

where  $k_2$  is the adsorption rate ( $\text{g/mg}\cdot\text{min}$ ),  $q_m$  is the adsorbate amount adsorbed onto the adsorbent in equilibrium (mg/g),  $q_t$  is the dye amount adsorbed at any time (mg/g).

The adsorption process can include several stages all with different adsorption rates. Every adsorption stage is governed by a different adsorption mechanism. An initial sharp region in intraparticle diffusion plots can emerge as a result of instantaneous adsorption or external surface adsorption caused by electrostatic attraction. This is followed by a second region in which intraparticle diffusion is accountable for restricting the adsorption rate. A third region occurs at the equilibrium state in cases where the intraparticle diffusion is restricted due to low adsorbate contents remaining in the solution (Allafchianet *al.*, 2019).

The testing of intra-particle diffusion possibility as a rate limiting step was performed using the IPD model, the equation of which is given Eq. (11);



$$q_t = k_{ipd}t^{0.5} + C \tag{11}$$

where  $k_{ipd}$  is the IPD rate constant. A plot of  $q_t$  versus  $t^{0.5}$  for different MB concentrations yielded two phases of the linear plots.

PFO, PSO, and IPD kinetic model parameters of MB adsorption on PCP are given in Table 5. The experimental results showed that the  $R^2$  coefficients were higher than 0.99 and that the experimental and analyzed  $q_e$  values were very close to each other. Results are shows that this separation process is suitable for the PSO kinetic model. The experimental and calculated  $q_e$  values for 318 K were higher than those for 298K and 308K. According to the tables herein, it is obvious that the  $q_e$  values increased with the increase in MB concentration. The comparison of the kinetic constants showed that the constant values were closer to both temperatures and concentrations of the PSO model. This result revealed that MG adsorption kinetics onto PCP resulted from PSO.

**Table 5.** PFO, PSO and IPD kinetic model parameters for MB adsorption onto PCP

| Kinetic Model     | Temp (K) | Kinetic coefficients                | 100 (mg/l)                 | 150 (mg/l) | 200 (mg/l) | 250 (mg/l) | 300 (mg/l) |        |
|-------------------|----------|-------------------------------------|----------------------------|------------|------------|------------|------------|--------|
| PFO kinetic model | 298      | $q_{e \text{ exp}}$ (mg/g)          | 20.297                     | 27.961     | 33.701     | 41.701     | 47.621     |        |
|                   |          | $q_{e \text{ exp}}$ (mg/g)          | 20.778                     | 29.302     | 35.034     | 43.228     | 48.963     |        |
|                   |          | $q_{e \text{ exp}}$ (mg/g)          | 21.754                     | 29.974     | 35.728     | 43.936     | 50.701     |        |
|                   | 308      | $k_1$ (min <sup>-1</sup> )          | 0.0281                     | 0.0418     | 0.0567     | 0.0321     | 0.0455     |        |
|                   |          | $q_{\text{ecal}}$ (mg/g)            | 7.975                      | 5.438      | 12.591     | 21.713     | 21.211     |        |
|                   |          | $R^2$                               | 0.8097                     | 0.7292     | 0.8696     | 0.8568     | 0.8854     |        |
|                   |          | $k_1$ (min <sup>-1</sup> )          | 0.0243                     | 0.0268     | 0.0465     | 0.0278     | 0.0442     |        |
|                   |          | $q_{\text{ecal}}$ (mg/g)            | 5.253                      | 10.610     | 21.431     | 18.857     | 27.004     |        |
|                   |          | $R^2$                               | 0.8443                     | 0.8325     | 0.8375     | 0.8124     | 0.8089     |        |
|                   |          | 318                                 | $k_1$ (min <sup>-1</sup> ) | 0.0399     | 0.0248     | 0.0297     | 0.0174     | 0.0169 |
|                   |          |                                     | $q_{\text{ecal}}$ (mg/g)   | 14.430     | 16.029     | 9.953      | 7.278      | 17.326 |
|                   |          |                                     | $R^2$                      | 0.8518     | 0.8362     | 0.8662     | 0.7806     | 0.8009 |
| PSO kinetic model | 298      | $k_2$ (min <sup>-1</sup> )          | 0.0335                     | 0.0257     | 0.0209     | 0.0199     | 0.0185     |        |
|                   |          | $q_{\text{ecal}}$ (mg/g)            | 20.704                     | 28.249     | 34.014     | 41.841     | 48.309     |        |
|                   |          | $R^2$                               | 0.9996                     | 0.9998     | 0.9999     | 0.9998     | 0.9998     |        |
|                   | 308      | $k_2$ (min <sup>-1</sup> )          | 0.0239                     | 0.0181     | 0.0149     | 0.0147     | 0.0135     |        |
|                   |          | $q_{\text{ecal}}$ (mg/g)            | 21.097                     | 30.488     | 35.842     | 44.053     | 49.751     |        |
|                   |          | $R^2$                               | 0.9997                     | 0.9993     | 0.9987     | 0.9994     | 0.9997     |        |
|                   | 318      | $k_2$ (min <sup>-1</sup> )          | 0.0196                     | 0.0141     | 0.0106     | 0.0096     | 0.0031     |        |
|                   |          | $q_{\text{ecal}}$ (mg/g)            | 22.173                     | 30.395     | 36.101     | 44.053     | 51.282     |        |
|                   |          | $R^2$                               | 0.9993                     | 0.9988     | 0.9999     | 0.9999     | 0.9991     |        |
| IPD kinetic model | 298      | $k_{id}$ (mg/g.min <sup>0.5</sup> ) | 0.7315                     | 0.9251     | 1.0329     | 1.3567     | 1.6073     |        |
|                   |          | $C$ (mg/g)                          | 11.578                     | 17.409     | 21.871     | 25.298     | 28.792     |        |
|                   |          | $R^2$                               | 0.5292                     | 0.4122     | 0.4004     | 0.4569     | 0.4752     |        |
|                   | 308      | $k_{id}$ (mg/g.min <sup>0.5</sup> ) | 0.7492                     | 1.2123     | 1.2809     | 1.5069     | 1.7196     |        |
|                   |          | $C$ (mg/g)                          | 12.129                     | 15.547     | 19.823     | 24.521     | 28.235     |        |
|                   |          | $R^2$                               | 0.5107                     | 0.7418     | 0.5371     | 0.5363     | 0.5199     |        |
|                   | 318      | $k_{id}$ (mg/g.min <sup>0.5</sup> ) | 0.7667                     | 1.1427     | 1.2943     | 1.3904     | 1.8391     |        |
|                   |          | $C$ (mg/g)                          | 12.323                     | 13.066     | 22.131     | 27.167     | 27.022     |        |
|                   |          | $R^2$                               | 0.5405                     | 0.7099     | 0.4488     | 0.4345     | 0.5851     |        |

### Conclusions

This study investigated MB adsorption onto PCP. The data obtained demonstrate that MB adsorption increased with the increase in initial dye concentration, contact time, and temperatures. The dye adsorption capacity onto PCP changed from 40.99 to 95.24 mg/g, 41.56 to 97.93 mg/g, and 43.51 to 101.41 mg/g for 298K, 308K and 318K, respectively, while the initial MB concentration increased from 100 to 300 mg/l. For the removal of dye the equilibrium adsorption time was fixed to 100 min. Pine cones are significant to develop the processes of adsorption and separation. The high adsorption capacity of pine cones depends on chemical reactivity and the porosity of the functional groups on its surface. These functional groups which bind the molecules on the pine cones have been investigated in



previous studies. Although natural and modified PCP used in some previous studies as a biosorbent, the type of PCP used in this study is different.

The isotherm studies carried out the present study indicated that the Freundlich model presented a more suitable profile for MB adsorption onto PCP compared to the Langmuir and Temkin models. It was noted that the parameters of these three isotherm models increased with the increment in temperature and that adsorption was acceptable at higher temperatures. The  $R^2$  values of all three isotherm models were found to be high. However, those of the Freundlich model were higher than the other two models. The monolayer adsorption capacity ( $q_m$ ) of PCP was determined as 65.36, 66.67, and 68.52 mg/g for 298K, 308K, and 318K, respectively.

The kinetic studies determined that the rate-limiting step could be dye chemisorption. The  $R^2$  coefficients were higher than 0.99 and the experimental and evaluated  $q_e$  values very close to each other. The kinetic constants were near to the temperatures and the concentrations. The  $q_e$  values increased with the increase in MB concentration. The IPD constant ( $k_{id}$ ) and monolayer concentration (C) values increased in line with the increase in temperature, revealing MB adsorption onto PCP.

The thermodynamic parameters demonstrate that MB adsorption onto PCP was endothermic. The absolute values of  $\Delta G^\circ$  decreased as temperature increased, proving that the separation process was constructive at low temperatures. The positive  $\Delta S^\circ$  value established an enhanced randomness in the solid-solute interface and the affinity of PCP for MB. In conclusion, all these results indicated that PCP may be used as an adsorbent for cationic dyes removal in wastewaters.

**Information About Paper:** *This study did not receive any specific grant from funding agencies in the public, commercial, or not-for-profit sectors. The authors declare that there is no conflict of interest regarding the publication of this paper.*

## References

- Allafchian A, Mousavi ZS, Hosseini SS, (2019) Application of cress seed mucilage magnetic nanocomposites for removal of methylene blue dye from water, *Int. J. Biol Macromol.* **136**, 199-208.
- Bedin KC, Martins, AC, Cazetta, AL, Pezoti, O, Almeida VC, (2016) KOH-activated carbon prepared from sucrose spherical carbon: Adsorption equilibrium, kinetic and thermodynamic studies for methylene blue removal. *Chem. Engin. J.*, **286**, 476-484.
- Caparkaya D, Cavas L, (2008) Biosorption of methylene blue by a brown alga *Cystoseira barbatula* Kutzing. *Acta Chimia Slovakia*, **55**, 547-553.
- Cherifi H, Fatiha B, Salah H, (2013) Kinetic studies on the adsorption of methylene blue onto vegetal fiber activated carbons. *Appl. Surf. Sci.*, **282**, 52-59.
- Crini G, (2006) Non-conventional low-cost adsorbents for dye removal: A review. *Biores. Tech.*, **97**(9), 1061-1085.
- Dawood S, Sen TK, (2012) Removal of anionic dye Congo red from aqueous solution by raw pine and acid-treated pine cone powder as adsorbent: equilibrium, thermodynamic, kinetics, mechanism and process design. *Water Res.* **46**(6), 1933-46.
- Debnath S, Ballav N, Maity A, Pillay K, (2017) Competitive adsorption of ternary dye mixture using pine cone powder modified with  $\beta$ -cyclodextrin. *J. Molecular Liquids*, **225**, 679-688.
- Demirak A, Keskin F, Şahin Y, Kalemci V, (2015) Removal of ammonium from water by cone powder as biosorbent. *Mugla J. Sci. & Tech.*, **1**(1), 5-12.
- El-Sikaily A, Khaled A, El-Nemr A, Abdelwahab O, (2006) Removal of methylene blue from aqueous solution by marine green alga *Ulva lactuca*. *Chemical Ecology*, **22**(2), 149-157.
- Forgacs E, Cserhati T, Oros G, (2004) Removal of synthetic dyes from wastewaters: *A Rev. Environ. Int.*, **30**, 953-971.
- Fu Y, Viraraghavan T, (2000) Removal of a dye from an aqueous solution by the fungus *Aspergillus niger*. *Water Quality Res. J.*, **35**(1), 95-111.
- Ghaedi M, Hajjati S, Mahmudi Z, Tyagi I, Agarwal S, Maity A, Gupta VK, (2015) Modeling of competitive ultrasonic assisted removal of the dyes – methylene blue and safranin-O using Fe<sub>3</sub>O<sub>4</sub> nanoparticles. *Chem. Engine. J.*, **268**, 28-37.

- Gouamid M, Ouahrani MR, Bensaci MB, (2013) Adsorption equilibrium, kinetics and thermodynamics of methylene blue from aqueous solutions using date palm leaves. *Energy Procedia*, (36), 898-907.
- Gupta VK, Suhas, (2009) Application of low-cost adsorbents for dye removal – A review. *J. Environ. Manage.*, **90**, 2313-2342.
- Hamed MM, Ahmed IM., Metwally SS, (2014) Adsorptive removal of methylene blue as organic pollutant by marble dust as eco-friendly sorbent. *J. Ind. Eng. Chem.*, **20**, 2370-2377.
- Immaculate LA, Ouma EBN, Ofomaja AE, (2018) Thermodynamic, kinetic and spectroscopic investigation of arsenite adsorption mechanism on pine cone-magnetite composite. *J. Environ. Chem. Engine.*, **6**, 5409-5419.
- Jian Z, Qingwei P, Meihong N, Haiqiang S, Na L, (2013) Kinetics and equilibrium studies from the methylene blue adsorption on diatomite treated with sodium hydroxide. *Appl. Clay Sci.*, **83**, 12-16.
- Jin Y, Zeng C, Lü QF, Yu Y, (2019) Efficient adsorption of methylene blue and lead ions in aqueous solutions by 5-sulfosalicylic acid modified lignin. *Int. J. Biol. Macrom.*, **123**, 50-58.
- Kausar A, Iqbal M, Javeda A, Aftab K, Nazli ZH, Bhatti HN, Nouren S, (2018) Adsorption Using Clay and Modified Clay: A Review. *Journal of Molecular Liquids*, **256**, 395-407.
- Kul AR, Aldemir A, (2019) Comparison of Methylene Blue Adsorption Performance on Natural, Thermal and Acid Modified Kaolin: Isotherm, Kinetics and Thermodynamics Studies. *Fres. Environ. Bull.*, **28**(6), 4475-4483.
- Kul AR, Koyuncu H, (2010) Adsorption of Pb(II) ions from aqueous solution by native and activated bentonite: Kinetic, equilibrium and thermodynamic study. *J Hazard Mater*, **179**, 332-339.
- Kupeta AJK, Naidoo EB, Ofomaja AE. (2018) Kinetics and equilibrium study of 2-nitrophenol adsorption onto polyurethane cross-linked pine cone biomass. *J. Cleaner Produc.*, **179**, 191-209.
- Mahmoodi NM, Hayati B, Arami M, Lan C, (2011) Adsorption of textile dyes on pine cone from colored wastewater: kinetic, equilibrium and thermodynamic studies. *Desalin.* **268**(1-3), 117-125.
- Martin-Lara MA, Blazquez G, Calero M, Almendros AI, Ronda A, (2016) Binary biosorption of copper and lead onto pine cone shell in batch reactors and in fixed bed columns. *International J. Mineral Proces.* **148**, 72-82.
- Miyah Y, Lahrichi A, Idrissi M, Khalil A, Zerrouq F, (2018) Adsorption of methylene blue dye from aqueous solutions onto walnut shells powder: Equilibrium and kinetic studies *Surfaces & Interf.*, **11** (1), 74–81.
- Mtshatsheni KNG, Ofomaja AE, Naidoo EB, (2019) Synthesis and optimization of reaction variables in the preparation of pinemagnetite composite for removal of methylene blue dye. *South African J. Chem. Engin.*, **29**, 33-41.
- Ofomaja AE, Naidoo EB, Modise SJ, (2009) Removal of copper(II) from aqueous solution by pine and base modified pine cone powder as biosorbent. *J Hazard Mater*, **168** (2-3), 909-17.
- Ofomaja AE, Naidoo EB, Modise SJ, (2010) Biosorption of copper(II) and lead(II) onto potassium hydroxide treated pine cone powder. *J. Environ Manage*, **91**(8), 1674-85.
- Ofomaja AE, Naidoo EB, (2010) Biosorption of lead(II) onto pine cone powder: Studies on biosorption performance and process design to minimize biosorbent mass. *Carbohydrate Polymers*, **82**(4), 1031-1042.
- Rafatullah M, Sulaiman O, Hashim R, Ahmad A, (2010) Adsorption of methylene blue on low-cost adsorbents: a review. *J Hazard Mater*, **177**(1-3), 70-80.
- Rida K, Bouraoui S, Hadnine S, (2013) Adsorption of methylene blue from aqueous solution by kaolin and zeolite. *Appl. Clay Sci.*, **83**, 99-105.
- Salleh MAM, Mahmoud DK, WAW, AbdulKarim A, Idris A, (2011) Cationic and anionic dye adsorption by agricultural solid wastes: A comprehensive review. *Desalin.*, **280**(1-3), 1-13.
- Yagub MT, Sen TK, Afroze S, Ang HM, (2014) Dye and its removal from aqueous solution by adsorption: a review. *Adv Collo. Inter.e Sci*, **209**, 172-84.